Analysis of nonuniform gratings

Neil G. R. Broderick and C. Martijn de Sterke
School of Physics and Optical Fibre Technology Centre, University of Sydney, New South Wales 2006, Australia
(Received 14 February 1995)

It has been shown earlier that the launching of gap solitons into nonuniform nonlinear Bragg gratings can be significantly easier than for uniform nonlinear Bragg gratings. In this paper we examine a variety of simple nonuniform Bragg gratings and compare their suitability for the launching process, by studying the positions of the zeros of the reflection spectrum.

PACS number(s): 42.70.Nq, 42.65.Hw, 42.50.Rh, 42.50.Ne

I. INTRODUCTION

In this paper we consider light propagating through nonuniform Bragg gratings in a direction orthogonal to the grating rulings, such as, for example, in fiber gratings, or in thin-film stacks. Previous work on nonuniform Bragg gratings concentrated on either the electric field profiles inside the Bragg grating, or on the general aspects of the reflection spectrum [1]. However, since the reflection spectrum can be written as the ratio of two analytic functions, it can be described completely by the positions of its poles and zeros in the complex frequency plane. If we continuously deform the Bragg grating, it is to be expected that the zeros and poles move continuously in the plane. Such trajectories are the focus of our paper as they provide new insight into the properties of nonuniform Bragg gratings.

We have earlier found that the launching of gap solitons [2–4] can be improved by using frequencies associated with the complex zeros of nonuniform Bragg gratings [5,6]. Since at a zero no light is reflected, the coupling of energy into the grating is most efficient at these frequencies. A zero in the reflection spectrum corresponds to a resonance inside the Bragg grating. The peak intensity at such a resonance can be much higher than the intensity outside the Bragg grating. As most optical nonlinearities increase with intensity, such resonances enhance these effects and thus allow them to be observed at lower powers than for a uniform structure. Which types of complex zeros are the best to use is the subject of this paper.

A complex frequency $\omega = \omega_r + i\omega_i$ implies that the electric field is growing exponentially at a rate given by ω_i. This can occur in two different ways. The first is that at a frequency ω_r the material has a gain or loss proportional to ω_i, which occurs when, for example, dealing with a laser problem. The other is that ω_i describes the exponential growth or decay of an external signal as occurs, for example, when dealing with pulses incident on the structure. Thus when using such zeros to launch gap solitons where vanishing reflection is required it is necessary to use pulses whose leading edge increases exponentially. The simplest such pulse is the hyperbolic secant shaped pulse, on which we have focused previously [5,6].

In possible experiments to launch gap solitons, the pulse width of the laser and hence of the input pulse is usually fixed and this determines ω_i. The best value of ω_r is determined by a number of factors [4,6]. The power needed to create a gap soliton increases as the frequency moves closer towards the bottom (top) of the band gap for a material with a positive (negative) nonlinearity. Thus the maximum power available from the laser sets a limit on the possible frequencies. If the frequency is too close to the band edge, then the gap soliton is no longer manifestly nonlinear as significant amounts of energy would be transmitted in the linear limit as well.

Thus in choosing the best grating for possible experiments it is necessary to know the position of its zeros in the complex frequency plane. In a previous paper [6] we simply assumed that we could always find a suitable zero. Using this assumption we were able to provide estimates for the power needed to create a gap soliton. In our previous work we considered step gratings and did not evaluate other grating types.

In contrast this paper describes the positions of complex reflection zeros for three types of nonuniform gratings. Each grating type is the concatenation of two uniform gratings. These have been chosen as they are the simplest nonuniform gratings to analyze and to fabricate. The purpose of the front grating is to facilitate the launching of the gap soliton, which then propagates through the back grating. The length of the front grating is thus roughly the length of the gap soliton we are trying to launch, while the back grating is much longer to allow a reasonable propagation distance. For each nonuniform grating we give a general description of the zeros, with an emphasis on the zeros which are relevant to launching gap solitons. We then discuss the suitability of each grating for the launching of gap solitons.

II. COUPLED MODE ANALYSIS

A Bragg grating couples light moving in opposite directions. This coupling is strongest at frequencies near the Bragg frequency ω_0. Thus we only need concentrate on the forward and backward propagating modes at frequencies close to ω_0. Also we make the slowly varying approximation and ignore rapid time oscillations. The slowly varying envelopes of the forward and backward

traveling modes are denoted by $\mathcal{F}_+$ and $\mathcal{F}_-$, respectively. The only other parameters are κ, the grating strength per unit length of the grating and hence the strength of the coupling, and δ, a normalized complex frequency which describes how close the frequency is to the Bragg resonance (at $\delta = 0$). For the gratings we consider both δ and κ are piecewise constant. In each section the linear coupled mode equations can then be written as [7]

$$\frac{\partial}{\partial z}\begin{pmatrix}\mathcal{F}_+(z)\\ \mathcal{F}_-(z)\end{pmatrix} = \begin{pmatrix} i\delta & i\kappa \\ -i\kappa & -i\delta\end{pmatrix}\begin{pmatrix}\mathcal{F}_+(z)\\ \mathcal{F}_-(z)\end{pmatrix}, \tag{1}$$

where [7]

$$\kappa = \frac{\pi\Delta n}{\lambda}, \quad \delta = \frac{\omega-\omega_0}{v_g}, \tag{2}$$

Δn is the maximum refractive index change in the grating, λ is the wavelength of the incident light, and v_g is the group velocity. As noted above, both ω and δ can be complex.

Equation (1) is solved by exponentiation, yielding the transfer matrix M:

$$M = \frac{1}{\beta}\begin{pmatrix} i\delta\sin\beta z + \beta\cos\beta z & i\kappa\sin\beta z \\ -i\kappa\sin\beta z & \beta\cos\beta z - i\delta\sin\beta z\end{pmatrix}, \tag{3}$$

where $\beta^2 = \delta^2 - \kappa^2$. In terms of M the solutions to the coupled mode equations are

$$\begin{pmatrix}\mathcal{F}_+(z)\\ \mathcal{F}_-(z)\end{pmatrix} = M\begin{pmatrix}\mathcal{F}_+(0)\\ \mathcal{F}_-(0)\end{pmatrix} \tag{4}$$

together with the boundary conditions,

$$\mathcal{F}_+(l) = 1 \quad \text{and} \quad \mathcal{F}_-(l) = 0, \tag{5}$$

where l is the length of the grating. These boundary conditions reflect the assumption that light is only incident upon the grating from the front ($z = 0$).

The amplitude reflection coefficient $r(\delta)$ is given by

$$r(\delta) = \frac{\mathcal{F}_{-(0)}}{\mathcal{F}_{+(0)}} = \frac{-M_{21}}{M_{22}}. \tag{6}$$

For a uniform grating the band gap lies between $-\kappa < \delta < \kappa$ where the reflection approaches unity, while outside the band gap the reflection decreases.

The zeros of the reflection spectrum are found by solving $r(\delta) = 0$ for δ. All the zeros of a uniform grating are real and occur at detunings given by [8]

$$\delta = \pm\frac{1}{l}\sqrt{\kappa^2 l^2 + n^2\pi^2}, \tag{7}$$

where n is a positive integer. In contrast, for nonuniform gratings analytic expressions for the zeros cannot usually be found.

By concatenating several uniform gratings, we obtain a nonuniform grating, whose field profile can be found by simply multiplying the separate transfer matrices together. If $M(i)$ denotes the transfer matrix for the ith uniform grating, then the matrix M is given by

$$M = M(n)\,M(n-1)\cdots M(i)\cdots M(2)\,M(1). \tag{8}$$

The reflection coefficient is still given by Eq. (6). Such nonuniform gratings form the focus of our paper, as unlike most grating structures their reflection spectrum can be found analytically.

For each detuning δ we can find the field distribution inside the grating; at a reflection zero the grating acts as a resonator and hence the peak field intensity inside the grating is higher than the intensity outside the grating. This resonance effect allows efficient launching of gap solitons using the complex zeros of nonuniform gratings.

Each of the nonuniform gratings we are interested in can be obtained by deforming a uniform grating. For these nonuniform gratings we can write the reflection spectrum as $r(\delta, x)$, where δ is the detuning and x is some parameter which describes the nonuniformity. Typically $x = 0$ corresponds to a uniform grating. If $\delta = \delta_0$ is a reflection zero at $x = x_0$, then if we vary x slightly we would expect the zero to move slightly. In fact the zero follows a trajectory given by

$$\frac{d\delta}{dx} = -\frac{\frac{\partial r}{\partial x}}{\frac{\partial r}{\partial \delta}}, \tag{9}$$

where r follows from Eq. (6). This method for following a zero is only useful if we know a point on the trajectory. For a uniform grating all the zeros are given by Eq. (7) and hence at $x = 0$ we know the initial point of the trajectories. In the sections below we utilize this method to determine whether or not particular gratings are useful for the launching of gap solitons.

A. Step gratings

Step gratings consist of two uniform gratings, each with a different κ and length l, but with the same Bragg frequency. Figure 1 shows the band diagram [8] for the step grating. The band gap for each grating is the shaded region in the diagram between $-\kappa$ and κ. Light incident upon the grating at these detunings is strongly reflected. We consider that κ_2 and l_2 are fixed, and vary the strength and length of the front grating in order to obtain suitable reflection zeros. In our previous paper

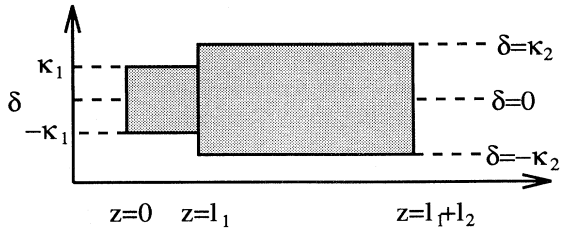

FIG. 1. Band diagram of a step grating. The front grating has a length l_1 and a strength κ_1. The main grating has a length l_2 and a strength κ_2.

we obtained estimates for the power required to launch gap solitons in these gratings, however here we wish to describe the position of the zeros in more detail.

From Fig. 1 it can be seen that when $\kappa_1 = 0$ or $\kappa_1 = \kappa_2$ then the step grating reduces to a uniform grating. In these cases we know that all the zeros must lie on the real axis at positions given by Eq. (7). When, however, κ_1 takes on intermediate values the zeros are in general complex. Equation (9) allows us to track a zero as $\kappa_1 = \kappa_2$ to $\kappa_1 = 0$. Since no new zeros are created as we vary κ_1 this method gives us knowledge about the positions of the zeros of the step grating, for when $\kappa_1 = \kappa_2$ they all lie on the real axis at detunings given by Eq. (7). This method can be used whenever we can obtain the required nonuniform grating by deforming a uniform grating. The trajectories obtained in this way possess features discussed below. Many of these can be understood with the help of the following theorem concerning the real zeros of the step grating.

Theorem 1. If a real frequency δ is a reflection zero of the two uniform gratings, then δ is a real reflection zero of the compound structure.

A proof of theorem 1 is as follows. If δ is a zero of the two uniform gratings, then $M(1)_{21} = M(2)_{21} = 0$, where $M(1)$ and $M(2)$ are the transfer matrices for each uniform grating. The $[2,1]$ element of the product is hence also zero and thus by Eq. (6) $r = M_{21}/M_{22} = 0$. It should be noted that when $\kappa_2 \neq \kappa_1$ the converse is also true. We are now able to discuss the trajectories in more detail.

For the step gratings there are two types of trajectories. The first of these occurs when a zero begins and ends on the real axis as κ_1 varies from κ_2 to 0. The second is when a zero goes to infinity as $\kappa_1 \to 0$. A typical trajectory of each sort is shown in Fig. 2. In Fig. 2(a) the zero is initially at the fifth zero of the large structure and it ends up at the third zero of the back grating when $\kappa_1 = 0$. If the zero's trajectory remains bounded, then the trajectory must end on the real axis at a zero of the back grating given by Eq. (7). By following the trajectories of all the zeros and noting where they land we can obtain a mapping from $\mathbb{Z}$ to $\mathbb{Z}$, however we have not been able to find a closed form analytic expression for this mapping. Hence we cannot predict where a particular zero's trajectory will finish.

For zeros that remain bounded as in Fig. 2(a), the main features of their trajectories are the "loops" and "bounces" that occur when the zero returns to the real axis. These features can be understood as follows. As κ_1 decreases the zeros of the front grating move in towards the origin along the real axis [see Eq. (7)], while the zeros of the back grating remain fixed. By theorem 1 whenever the zeros of the two gratings match up, the step grating has a real zero and hence one of the trajectories must return to the real axis. It should be noted that such trajectories in general remain outside the band gap and hence are of no use in launching gap solitons. Instead we must look at the zeros which go to infinity as in Fig. 2(b).

Recall that when $\kappa_1 = \kappa_2$ or $\kappa_1 = 0$ we have a uniform grating and all the zeros lie on the real δ axis. Since at the beginning and end of the trajectories we have a uniform grating, the zeros can be put into a 1-1 correspondence with the positive integers [using Eq. (7)] and hence it is possible that all trajectories could begin and end on the real line, with no trajectories going to infinity. However most simple one-one pairings, such as the nth zero of the initial grating going to the nth zero of the final grating, would cause the length of the trajectories to increase without bound. The reason for this can be seen from Eq. (7), which shows that the spacing of the zeros for a uniform grating is asymptotically π/l. The initial and final distribution of zeros is shown in Fig. 3; note that the final distribution of zeros is less dense than the initial distribution and hence the distance between the nth zero of the initial grating and the nth zero of the final grating increases without limit as n increases. Instead of the length of all the trajectories increasing we find that the length of most zero's trajectories remains bounded, except for some for which $\delta_i \to \infty$. The fraction of zeros which goes to infinity appears to depend on the ratio of lengths of the two gratings. We are, however, unable to predict which zeros go to infinity. The zeros that go off to infinity have asymptotic trajectories given by

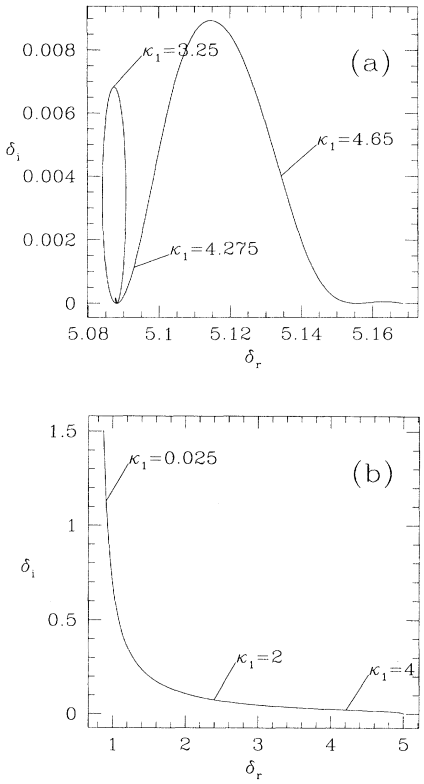

FIG. 2. Trajectories for a step grating with parameters $\kappa_2 = 5$, $0 < \kappa_1 < 5$, $l_1 = 2$, and $l_2 = 10$. (a) shows the trajectory for the $n = 5$ zero of the large grating which starts at $\delta = 5.169$ when $\kappa_1 = 5$ and finishes at $\delta = 5.088$ when $\kappa_1 = 0$. The value of κ_1 at some intermediate positions is shown on the graph. (b) shows the trajectory for the $n = 1$ zero of the large grating which starts at $\delta = 5.007$ and moves to the left as κ_1 decreases.

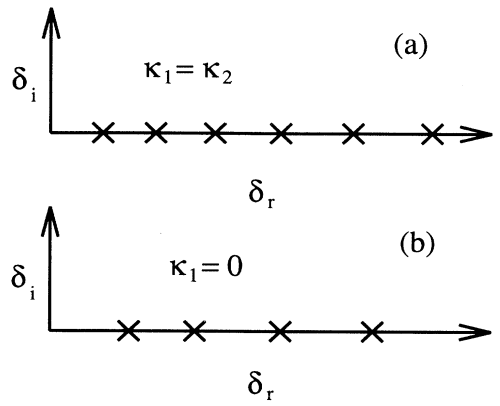

FIG. 3. The position of the zeros on the real axis. (a) shows the initial position of the zeros, and (b) shows the final point. Note that the density of zeros is higher in (a).

$$\delta(\kappa_1) = \frac{p\pi}{2l_1} + \frac{i}{2l_1} \ln \frac{\kappa_2 - \kappa_1}{\kappa_1}, \tag{10}$$

where p is a positive integer. Note that when $p = 1$, $\delta_r = \pi/(2l_1)$, which is less than κ_2 if l_1 is sufficiently large. Thus the trajectory of the first zero which goes to infinity can pass through the band gap. This can be seen in Fig. 2(b) where the trajectory approaches that given by Eq. (10) with $p = 1$. Numerical simulations show that this zero can be used to launch gap solitons, and that the power required can be less by a factor of 5 compared to the uniform case [6]. We have found that this zero corresponds to the first zero of the grating with $\kappa_1 = \kappa_2$. So when deciding which step grating is best to launch a gap soliton only the trajectory of the first zero needs to be considered.

B. Chirped gratings

The next nonuniform grating type we consider is the step chirped grating whose band diagram [8] is shown in Fig. 4. Here we have two gratings with the same strength but with a different length and Bragg frequency. This can be achieved by writing the second grating with a different period from the first. The difference between the two resonance frequencies is given by Δ while the actual frequency of the zero is given by δ with $\delta = 0$ corresponding to the Bragg frequency of the back grating. When $\Delta = 0$ the chirped grating reduces to a uniform grating with length $l_1 + l_2$. When the two gratings have very different Bragg frequencies, which corresponds to $\Delta \gg \kappa$, the two gratings are essentially independent as seen in Fig. 5, which shows the reflection spectrum for a chirped grating when the frequency difference Δ is much larger than the width of the gratings. In the extreme limit when $\Delta \to \infty$ the frequency difference is so large that the first grating has no effect and we can consider the chirped grating to be a uniform grating with length l_2. By varying Δ and following a particular zero we obtain trajectories similar to the ones described above. Typical such trajectories are shown in Fig. 6.

Again there are two sorts of trajectories, those which cross the band gap of the larger grating, and ones that loop about before settling down at the location of a zero of the back grating. The looping of the trajectories is again caused by the crossing of zeros of the front and back grating which force the trajectory back to the real axis. As Δ increases the trajectories that settle down are affected less by the front grating and move closer to the position of the zeros of the back grating given by Eq. (7). The zeros that continue to move with Δ also approach the real axis as the effect of the back grating decreases.

The trajectories that cross the band gap can be understood by examining the zeros of the two gratings separately. As Δ increases the zeros of the front grating all move to the left in Fig. 6 by the same amount. Eventually one of them enters the band gap of the larger grating. When this happens our numerical work suggests that a zero of the compound structure begins to cross the band gap. These trajectories go to infinity as Δ approaches infinity. Also since they pass through the band gap they can be used for launching gap solitons.

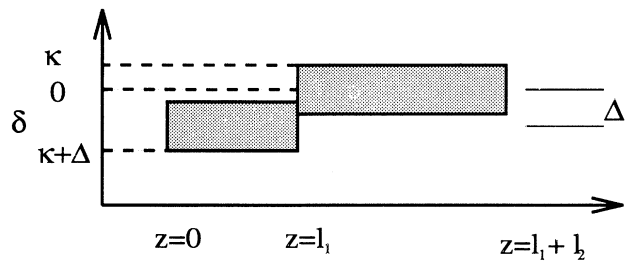

FIG. 4. Schematic of a chirp grating. The front grating has a length l_1 and a strength κ_1. The main grating has a length l_2 and a strength κ_2. The difference between the two Bragg frequencies is given by Δ.

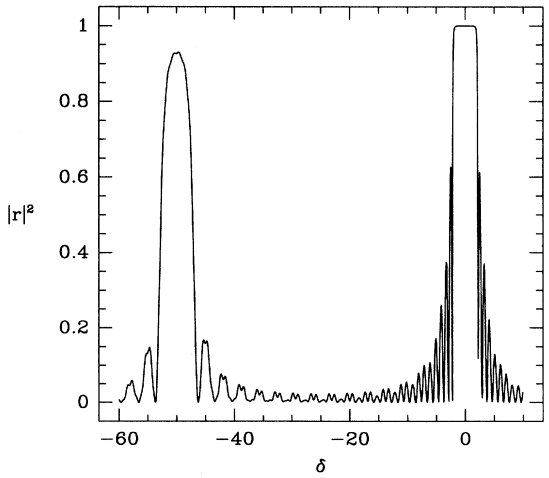

FIG. 5. Reflection spectrum of a chirped grating with $l_1 = 1\,\text{cm}$, $l_2 = 3\,\text{cm}$, $\kappa = 2\,\text{cm}^{-1}$, and $\Delta = 50\,\text{cm}^{-1}$. Note that the two reflection peaks are well separated and that close to either peak the reflection spectrum is essentially that of a single uniform grating.

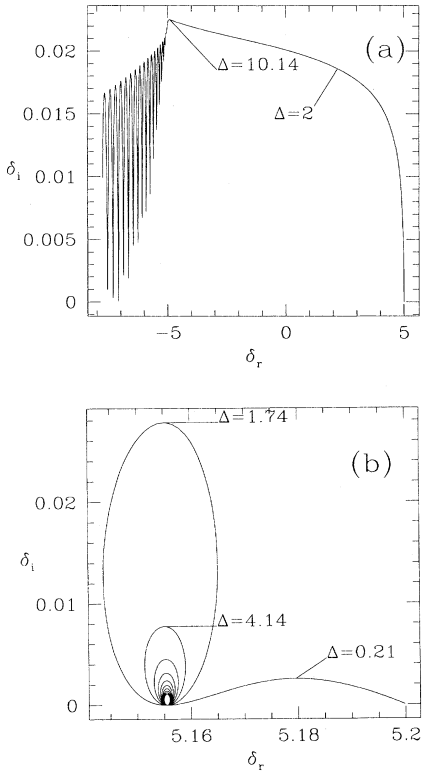

FIG. 6. Trajectories for a chirp grating with parameters $\kappa = 5$, $0 < \Delta < 13$, $l_1 = 1$, and $l_2 = 10$. (a) shows the trajectory of the $n = 1$ zero of the initial grating (when $\Delta = 0$) which starts at $\delta = 5.008$ and moves to the left. The rapid oscillations at the end of the trajectory are caused by the crossing of the zeros of the back grating. (b) shows the trajectory for the $n = 5$ zero of the initial grating. It begins at $\delta = 5.2$ and moves to the left finishing at $\delta = 5.155$ which corresponds to the $n = 4$ zero of the back grating.

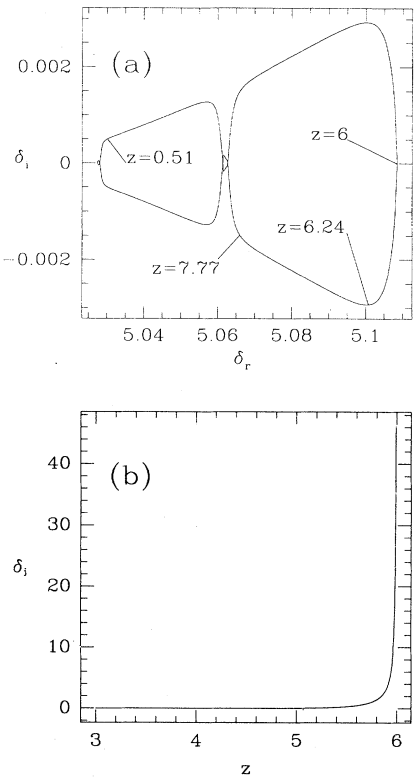

FIG. 7. Typical trajectories for a phase shifted grating. In (a) $\phi = 0.4\pi$, $l = 12$, and $0 < z < 12$ the trajectory starts and finishes at $\delta = 5.027$, which is the second zero of the uniform grating. Note that it returns to the real axis six times during the course of the trajectory; various values of z are shown on the graph. In (b) $\phi = 0.5\pi$, $l = 6$, and $3 < z < 6$. Here we show only the δ_i as a function of z. Initially $\delta_r = 0$ and it varies insignificantly as a function of z.

C. Point defects

The last nonuniform grating we consider consists of a uniform grating with parameters l and κ plus a point defect located at z where $0 < z < l$. The effect of the point defect is to change the phase of the electric field at that point. Such features are well known in the semiconductor laser literature, where they are used in some distributive feedback designs [9]. When the phase shift is located at the center of the grating, then the reflection spectrum has a zero at the center of the band gap. If the point defect is located at either the front or the back of the grating, then grating is uniform.

The transfer matrix for a point phase shift is a diagonal matrix with diagonal elements $\exp(i\phi)$ and $\exp(-i\phi)$. The phase shift ϕ can take any value from 0 to π. When $\phi = \pi$ the transfer matrix becomes Diag$[-1, -1]$ and the reflection spectrum is thus unchanged. In order to find the positions of the zeros we start with the point defect located at either the front or the back of the grating and move the defect through the grating, while tracking the zeros. Figure 7(a) shows a trajectory as the position of the point defect moves through the grating. Its main feature is that the trajectory begins and ends at the same point. The reason for this is that the reflection spectrum for a lossless grating from one end is the complex conjugate of the spectrum at the other end. Consider a reflection spectrum $r(\delta, \phi, z)$ for a grating of length l, where ϕ is the phase shift caused by the point defect which is located at position z. If at $\delta = \delta_0$, $r(\delta_0, \phi, z) = 0$, then

$$r(\delta_0^*, \phi, l - z) = r(\delta_0^*, \phi, z)^* \tag{11}$$
$$= r((\delta_0^*)^*, \phi, z) \tag{12}$$
$$= r(\delta_0, \phi, z) \tag{13}$$
$$= 0. \tag{14}$$

In particular this implies that when $z = l/2$ all the zeros lie on the real δ axis. Hence once the point defect has passed halfway, the trajectory returns to its starting point by following the conjugate of its outward path. These trajectories remain outside the band gap and so cannot be used to launch gap solitons. To be able to use such gratings we need to find zeros which enter the band gap.

Whereas above all the zeros started on the real axis for the case of a phase shifted grating, some zeros start and

finish at infinity. One such zero is shown in Fig. 7(b). In contrast to previous plots which show the trajectory in the (δ_r, δ_i) plane, here we plot δ_i against the location of the point defect z. The reason for this is that $\delta_r = 0$ initially and when $z = l$, $\delta_r < 10^{-14}$. When the point defect is at the center of the grating the zero is on the real axis inside the band gap, but as the point defect moves towards the edge, the zero moves almost vertically away from the real axis. When the point defect is near the center of the grating we can get an approximate position for the zero by assuming that the grating is infinite. The case of an infinite grating with a phase defect at the origin can be solved exactly and leads to a resonance inside the band gap located at

$$\delta = \kappa \cos\phi. \tag{15}$$

For a finite grating this resonance becomes a reflection zero at the position very close to that given by Eq. (15). This approximation is most accurate for long gratings and when the point defect is closest to the center.

III. LAUNCHING ZEROS

In Sec. II we discussed the general properties of various nonuniform gratings. In this section we concentrate on the suitability of each type of grating for launching gap solitons. In particular we consider, if we have two gratings which have a zero at the same (complex) frequency, which grating is best to launch a gap soliton. To create a gap soliton efficiently two problems have to be overcome. The first of these, the "reflection problem," is that of coupling energy efficiently into the grating. The second of these, the "formation problem," is that the energy inside the grating must be able to form a gap soliton. Before discussing these in detail below, we note that the reflection problem depends only on the position of the reflection zeros in the complex frequency plane, i.e., δ_i must match the source pulse width (see Sec. I), while δ_r matches the frequency of the source. In contrast, the formation problem deals with the field distribution inside the grating, which not only depends on the position of the reflection zero, but also on the grating geometry. In particular the formation problem depends strongly on the width of the field distribution inside the grating. Of the two problems, solving the reflection problem is more crucial since the gap soliton cannot form if there is insufficient energy. However, the formation problem provides a criterion to rank different gratings which all solve the reflection problem.

We first turn to the reflection problem. For a zero to be suitable δ_i must match the temporal pulse width of the source. Specifically, for a hyperbolic secant shaped pulse the width T must equal $1/(\delta_i v_g)$ [6]. A typical pulse width for possible experiments is 100 ps, which corresponds to $\delta_i = 0.5\,\mathrm{cm}^{-1}$ in glass (with a refractive index $n = 1.5$). Similarly in an experiment the value of δ_r must match the frequency of the source. When designing the grating this consideration is somewhat relaxed since the entire reflection spectrum can be moved by about a nanometer by tuning the grating after it has been written [10]. Instead the value of δ_r is determined by the solution to the formation problem.

In solving the formation problem we rely on the following features of a gap soliton: (i) they are single peaked; (ii) their spatial width w_G and center frequency δ_r obey

$$\delta_r^2 + \frac{4}{w_G^2} = \kappa^2. \tag{16}$$

Earlier [6] we argued that a structure with a linear resonance which has the above features would be most efficient at launching a gap soliton. That is, we require the linear resonance also to be single peaked and to have a width $w_l = w_G$, and furthermore w_l and frequency δ_r of the zero to satisfy Eq. (16).

For a uniform grating, the intensity profile associated with the nth reflection zero has n local maxima. As we deform the grating and track the zeros this property remains. Since gap solitons have only a single intensity maximum we can therefore restrict our search to the first zero of nonuniform gratings. In general the width w_l of the resonance is a complicated function of the frequency of the zero and the geometry of the structure, and hence we treat it as an independent parameter in our problem. By requiring that w_l and δ_r satisfy Eq. (16) we thus fix the value of δ_r. We stress that T, the temporal width of the incoming pulse, and w_l, the spatial width of the linear resonance, are not related; for example, in a step grating $w_l \approx l_1$.

Thus for each grating we are concerned with the following three parameters: the real and imaginary part of the first zero and the spatial width w_l of the associated linear resonance.

For a step grating, finding zeros which lie on the ellipse given by Eq. (16) is a simple task. Figure 8 shows the positions of 8000 zeros in the $(\delta_r, 1/w)$ plane. Each zero is the first zero of a step grating with $\kappa_2 = 5$, $l_2 = 10$, and with κ_1 and l_1 uniformly distributed in the intervals $0 < \kappa_1 < 5$ and $0.5 < l_1 < 2$. Figure 8 shows only those zeros which are sufficiently close to the ellipse and satisfy $\kappa_2 - 1 < \delta_r < \kappa_2$ and $\delta_i < 1$. The solid line is the ellipse given by Eq. (16) where $\kappa = \kappa_2$. The value of κ for the back grating is used in drawing the ellipse since the gap soliton propagates through the back grating [6].

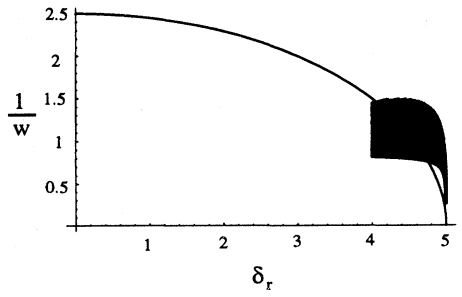

FIG. 8. Graph showing the position of various zeros on the $(\delta_r, 1/w)$ plane, along with the ellipse given by Eq. (16). Each point on the graph corresponds to the first zero of a step grating with $\kappa_2 = 5$, $l_2 = 10$, and $0 < \kappa_1 < 5$, $0.5 < l_1 < 2$.

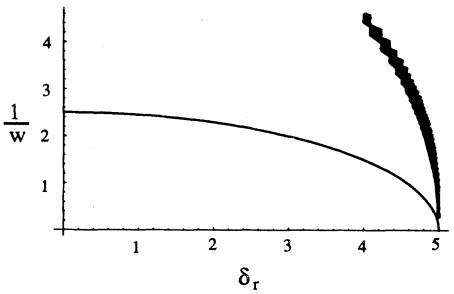

FIG. 9. Graph showing the position of various zeros on the $(\delta_r, 1/w)$ plane, along with the ellipse given by Eq. (16). Each point on the graph corresponds to a zero of a phase shifted grating with $\kappa = 5$, $l = 12$, and the position of the defect is between 0.5 and 2.

In addition, for the zeros of interest we have found that $\kappa_1 \approx \kappa_2$ and hence the ellipse is not significantly altered if we used κ_1 instead of κ_2. It is clear that the zeros cover a significant proportion of the ellipse, and hence we can easily find a suitable zero to launch a gap soliton. By changing the parameters of the grating slightly, while keeping κ_2 constant we can find zeros which cover nearly all of the ellipse. The imaginary parts of the zeros take on a wide range of values which means that finding zeros suitable for a wide range of pulse widths is possible.

For the chirped grating, finding suitable zeros is more complicated than for a step grating since the zeros that enter the band gap return to the real axis on the other side of the band gap, and thus δ_i tends to be smaller than for the step grating. This implies that for longer pulses a chirped grating would possibly be better than a step grating of the same length. The coverage of the $(\delta_r, 1/w)$ plane is not as complete as it is for a step grating, making it harder to find zeros which lie on the relevant ellipse.

For a phase shifted grating, $\mathcal{F}_+$ and $\mathcal{F}_-$ are discontinuous at a point defect, which means that the width of the resonance is generally narrower than it would be if it were continuous. Thus the zeros for a phase shifted grating would on the average lie above the zeros of either a step grating or a chirped grating in the $(\delta_r, 1/w)$ plane. Since the zeros of the other two gratings cover the relevant part of the ellipse, the zeros of the phase shifted gratings would be expected to be above the ellipse, and hence not suitable to launch gap solitons. In fact this is the case as can be seen in Fig. 9, where again $\kappa = 5$ and $l = 10$. This implies that the phase shifted grating is not suited for launching gap solitons.

IV. DISCUSSION

The launching of gap solitons in nonuniform gratings requires zeros in the reflection spectrum at particular complex frequencies. By tracking the zeros of a uniform grating as we deform it we are able to determine whether a particular grating is suitable. In addition the trajectories of the zeros themselves possess many interesting features, which can be easily seen using our approach.

Of the three gratings that we examined the best grating to use for launching gap solitons is the step grating, while the phase shifted grating is not suitable for launching gap solitons. The third grating type — the chirped grating — is suitable for experiments involving nanosecond pulses but is not as good as the step grating for shorter pulse lengths.

Step gratings differ from the other two grating types in that the total strength of the grating decreases as we deform it. This feature causes some of the trajectories to go to infinity, and hence we can find zeros which have high values for δ_i corresponding to short pulses. In contrast the zeros for the other two gratings hug the real axis and hence δ_i never increases sufficiently.

ACKNOWLEDGMENTS

This work was supported in part by the Australian Photonics CRC (APCRC) and by the Australian Research Council. The Optical Fibre Technology Centre is a member in the Australian Photonics CRC. N.G.R.B. is grateful for financial support from the APA.

[1] H. Kogelnik, Bell Syst. Tech. J. **55,** 109 (1976).
[2] H. G. Winful, J. H. Marburger, and E. Garmire, Appl. Phys. Lett. **35,** 379 (1979).
[3] W. Chen and D. L. Mills, Phys. Rev. Lett. **58,** 160 (1987).
[4] C. M. de Sterke and J. E. Sipe, in *Progress in Optics*, edited by E. Wolf, (North-Holland, Amsterdam, 1994), Vol. XXXIII, Chap. III, pp. 203–260.
[5] C. M. de Sterke and J. E. Sipe, Opt. Lett. **18,** 269 (1993).
[6] Neil Broderick, C. M. de Sterke, and J. E. Sipe, Opt. Commun. **113,** 118 (1994).
[7] C. M. de Sterke and J. E. Sipe, Phys. Rev. A **42,** 550 (1990).
[8] J. E. Sipe, L. Poladian, and C. M. de Sterke, J. Opt. Soc. Am. A **11,** 1307 (1994).
[9] G. P. Agrawal and N. K. Dutta, *Semiconductor Lasers*, 2nd ed. (ITP Van Nostrand Rienhold, New York, 1993).
[10] A. Meltz, W. W. Morey, and J. R. Dunphy, Proc. SPIE **1587**, 350 (1991).